Artigo

STUDY OF THE CHROMIUM(VI) REMOVAL FROM AQUEOUS SYSTEMS BY COBALT NANOPARTICLES

Patricia G. Leles[a], Mayra A. Nascimento[a], Jean C. Cruz[a], Paloma V. F. de Sousa[a] and Renata P. Lopes*[,a]
[a]Departmento de Química, Universidade Federal de Viçosa**,** 36570-000 Viçosa – MG, Brasil

Recebido em 10/02/2019; aceito em 11/04/2019; publicado na web em 08/05/2019

The cobalt nanoparticles (NPs-Co) were synthesized and applied in the removal of Cr(VI). The obtained nanomaterials presented magnetic properties and were characterized by the techniques of Transmission Electron Microscopy and X-ray diffraction. The NPs-Co, with a diameter of less than 50 nm, had a composition based on metallic cobalt and cobalt oxide. The NPs-Co were applied in the removal of Cr(VI) being evaluated different parameters such as time of equilibrium, initial pH, dose of NPs-Co, concentration of Cr(VI), and system temperature. The removal of Cr(VI) was favored at lower pH values, being about 100% at pH 2.0. With the increase of Cr(VI) concentration from 40.0 to 300.0 mg L^{-1} the removal decreased from 80 to 15%. The NPs-Co dose promoted an increase in removal reaching 90% at a dose of 1.0 g L^{-1}. The removal process was spontaneous and endothermic, and the Langmuir isotherm model fit better to experimental data. The maximum removal capacity was approximately 70.0 mg g^{-1}. The removal kinetics followed the pseudo-second order model. The mechanism of Cr(VI) removal occurred through adsorption by electrostatic interactions between CrO_4^{2-} anion and Co-NPs, followed by reduction of Cr(VI) to Cr(III) and, lastly, co-precipitation of Cr(III) as $Cr(OH)_3$ on the NPs-Co.

Keywords: Reduction; adsorption; co-precipitation; environmental contaminants.

INTRODUCTION

In recent years, due to the scarcity of drinking water, the water pollution sources have become a serious environmental problem. Among the pollutants present in aqueous environments, heavy metals are noteworthy, that includes chromium, mercury, cadmium, arsenic, thallium, zinc, nickel, copper, and lead. Some of these metals, in very small amounts play an essential role in human and animal metabolism, but in high concentrations can cause toxicity and health risks, as they are not biodegradable and are bioaccumulative in living organisms.[1]

Among the heavy metals, the chromium is classified as the highest priority toxic pollutant by USEPA (United States Environmental Protection Agency), because it is highly soluble and toxic to living organisms. The Cr(VI) is harmful to health due to it is teratogenic, mutagenic, and carcinogenic nature.[2] This element is heavily used in industries of metallurgy, mining, electroplating, leather tanning, polishing, pigments, and printing.[3] It can be released into the environment through the inadequate discharge of waste from these industries.

Due to the Cr(VI) toxicity, the new methods development that promote the removal of this element from water bodies is necessary. In the last years, materials at nanoscale have been studied for application in the removal of different environmental contaminants, in particular, metallic nanoparticles. Metal nanoparticles are materials that have higher surface energy, large surface area, small size, and high reactivity[4] which makes them promising in the removal of environmental contaminants.

In many works metallic nanoparticles are being used in the Cr(VI) removal[3, 5-7] either due to adsorptive and/or reductive processes, which reduce Cr(VI) in its less toxic Cr(III) form. Despite the promising results with the use of metallic nanoparticles disadvantages are described in the process. As for example, the difficult recovery of the nanoparticles after the removal process, which is hampered due to its nano size. Then, the magnetic nanoparticles are particular interest in the field of environmental contaminants removal, since they can be easily recovered by applying an external magnetic field, which has already been accomplished in many works.[2,8-10]

In particular, cobalt magnetic nanoparticles, besides the advantage of easy recovery after the process, have a high resistance to corrosion and wear. Besides that, are easily synthesized through the chemical reduction process, with the use of reducing agents such as sodium borohydride ($NaBH_4$).[8,11] Some works described the use of cobalt nanoparticles and also cobalt oxide in the environmental contaminants removal in aqueous media, with promising results.[8-10,12-14] However, there are no reports in the literature that use only Co nanoparticles in the removal of Cr(VI). Besides that, the mechanism of Cr(VI) removal by these nanomaterials is still not well understood. Thus, in this work, the magnetic nanoparticles of cobalt were synthesized by chemical reduction and applied in the removal of Cr(VI).

MATERIAL AND METHODS

Reagents and Solutions

The reagents used were nitric acid, potassium chromate, acetone, sodium hydroxide, and hydrochloric acid, all obtained from Merck. Cobalt(II) acetate tetrahydrate obtained from Dinâmica. Sodium borohydride obtained from Sigma-Aldrich. Ethanol (95%) obtained from Vetec. Sulfuric acid obtained from Synth. 1.5-Diphenylcarbazide obtained from Neon.

All solutions used were prepared from ultrapure water (system Milli-Q from Direct-Q 3UV) and stored under refrigeration at 4 °C.

Synthesis of Cobalt Nanoparticles (NPs-Co)

The NPs-Co were synthesized by chemical reduction of the metal using sodium borohydride (equation 1), with adaptations of the methodology reported by Liang and Zhao[8]. Initially 8.62 g of cobalt(II) acetate tetrahydrate was added to 50.0 mL of ethanol/water (4:1, v/v) solution. The system was kept under constant stirring for 10 min. After the time interval, 100.0 mL of sodium borohydride (1.08 mol L^{-1}) solution was added to the system at a

*e-mail: renata.plopes@ufv.br

rate of approximately 50.0 μL min^{-1} under constant stirring with the formation of a black precipitate. The system was allowed to stand at room temperature, and subsequently, vacuum filtration and washing of the material obtained with Milli-Q water and ethanol were performed. Finally, the material obtained was oven dried at 40 °C for approximately 2 hours and stored under refrigeration at -20 °C.

$$2Co^{2+}_{(aq)} + BH^{-}_{4(aq)} + 2H_2O_{(l)} \rightarrow 2Co^{0}_{(s)} + BO^{-}_{2(aq)} + 4H^{+}_{(aq)} + 2H_{2(g)} \quad (1)$$

Characterization of NPs-Co

Morphological characterization and particle size were performed using a Transmission Electron Microscopy (Tecnai G2-12 - SpiritBiotwin FEI - 120 kV). To evaluate the structure of NPs-Co was used an X-ray diffractometer (Bruker model D8 Discover, using radiation Cu-Kα (λ = 0.1541 nm) with angular variation 2θ from 5 to 95°) and Fourier Transform Infrared Spectroscopy (FT-IR 660, Varian Inc., EUA) in the region of 400 to 4000 cm^{-1}. To determine the pH of the point of zero charge (PZC) of nanomaterials, was added 20.0 mL of NaCl (0.050 mol L^{-1}) in six Erlenmeyer flasks, with initial pH set to 2.0, 4.0, 6.0, 8.0, 10.0 and 12.0 using solutions of HCl or NaOH (0.10 mol L^{-1}). Subsequently, 20.0 mg of NPs-Co were added to each Erlenmeyer flasks. The system was placed under constant orbital agitation (220 rpm, Incubator Shaker Series - New Brunswick Scientific) at 25 °C for 48 hours. After the time interval, the suspensions were centrifuged (3600 rpm) during 10 minutes and the final pH values of the supernatant were measured.[15] The pH value in the PZC was calculated by the arithmetic mean of the final pH points that were constant.[16]

Removal of Cr(VI) by NPs-Co

The removal assays were performed in Erlenmeyer flasks 125 mL, wherein 20.0 mL of Cr(VI) solution and the required dose of NPs-Co were added. The reactions were under constant agitation (220 rpm). At predetermined times (10 hours) aliquots were collected and filtered on PTFE membrane (0.45 μm and 13 mm diameter, Millipore). To quantify the remaining Cr(VI) in the solution, the colorimetric method of 1.5-diphenylcarbazide was used.[17] After the reaction, an aliquot of 500.0 μL of sample, previously filtered, was transferred to a 10.0 mL volumetric flask. 20.0 μL of concentrated H_2SO_4 and 200.0 μL of 1.5-diphenylcarbazide (8.25×10^{-3} mol L^{-1}) also were added to the flask. The volume was completed with Milli-Q water. The Molecular Absorption UV/Vis Spectrophotometry (Thermo Scientific - Model Evolution Array) in the wavelength of 542 nm was used to monitor the percentage of Cr(VI) removed.

Different parameters were evaluated in Cr(VI) removal by NPs-Co as: (1) time of equilibrium, dose of the NPs-Co (0.20, 0.40, 0.60, 0.80, 1.00, 1.60 and 2.00 g L^{-1}), initial concentration of Cr(VI) (40.0, 80.0, 100.0, 150.0, 200.0 and 300.0 mg L^{-1}), and initial pH (2.0, 4.0, 6.0, 8.0, 10.0 and 12.0). The pH adjustment was performed with solutions of HCl (0.10 mol L^{-1}) or NaOH (0.50 mol L^{-1}).

Kinetic studies were performed with the experimental data adjusted to kinetic models of pseudo-first-order (Lagergren)[18] and pseudo-second order (Ho e McKay).[19] Studies of adsorption isotherms were also performed by adjusting the experimental data to the Langmuir[20,21] and Freundlich[22] isotherm models.

The thermodynamic study was performed using Cr(VI) concentrations at 40.0, 80.0, 100.0, 150.0, 200.0 and 300.0 mg L^{-1}. For each of these concentrations, the tests were performed at temperatures of 15, 25, 35, 45 and 55 °C. At the end of the reactions, the samples were filtered and analyzed on the UV/Vis spectrophotometer.

The ability to remove Cr(VI) by NPs-Co, in a certain time interval, q_t (mg g^{-1}), and the rate of removal were calculated through equations 2 and 3, respectively.

$$q_t = \frac{(C_0 - C_t)V}{m} \quad (2)$$

$$\% \text{ removal} = \frac{(C_0 - C_t) \times 100}{C_0} \quad (3)$$

wherein C_t is the residual concentration of Cr(VI) (mg L^{-1}) in time t (min) and C_0 is the initial concentration of Cr(VI) in the solution (mg L^{-1}), V it is the volume (L), and m is the mass of nanoparticles (g).

The Cr(III) and Cr(VI) adsorbed in the nanoparticles was investigated after the Cr(VI) removal reaction by Co-NPs. Then, the NPs were digested with concentrated HNO_3. For this, after the reaction, the solution was centrifuged and the Co-NPs were deposited on the bottom of the flask. Nanoparticles recovered in the previous step made the addition of 3.0 mL water and 2.00 mL HNO_3 concentrated. The mixture was heated to a temperature of about 200 °C until complete dissolution. After this procedure, the solution was transferred to a 10.00 mL flask and the volume filled with Milli-Q water. Cr(VI) was quantified by the 1.5-diphenylcarbazide method as described above, while Cr (III) was quantified by the EDTA method. For this, in 4.0 mL of the resulting solution was added 500.0 μL of EDTA solution (0.10 mol L^{-1}), 1.0 mL of acetate buffer (0.18 mol L^{-1}, pH 4.0), and 2.00 mL Mili-Q water. The system was heated in a water bath (80 °C) for 30 minutes and then cooled with ice. The resulting solution was analyzed by Molecular Absorption UV/Vis Spectrophotometry (λ = 543 nm).

All assays were performed in triplicate.

Desorption assays of Cr(VI) and reuse of NPs-Co

At the end of the reaction ($C_{Cr(VI)}$ = 40.0 mg L^{-1}, dose of NPs-Co = 1.0 g L^{-1}, 25 °C), the solution was centrifuged and the supernatant was removed. Then, 20.0 mL of NaOH solution (0.10 mol L^{-1}) was added on nanoparticles and thereafter was stirred for 10 hours. After the time interval, the system was filtered and diluted in one ratio 1:3 (solution:water, v/v). The quantification of the remaining Cr(VI) was analyzed by Atomic Absorption Spectrophotometry with flame (Shimadzu, model AA-6701F, with Burner-atomiser "flame-type" Acetylene/Air – 2250 °C).

For the reuses of the NPs-Co, after desorption, the nanoparticles were washed and added to the solution of Cr(VI) (40 mg L^{-1}). The system was kept under stirring for 10 hours. Two consecutive adsorption/desorption cycles were performed in NaOH. The rate of Cr(VI) removal by Co-NPs was analyzed by UV/Vis spectrophotometry, with wavelength monitoring at 542 nm.

RESULTS AND DISCUSSION

Characterization of NPs-Co

The synthesized NPs-Co presented a black coloration and magnetic properties since they can be quickly attracted by a magnetic bar to the glass wall, demonstrating its magnetic characteristic (Figure 1S in Supplementary Material). The magnetic properties of the NPs-Co allow them to be easily separated using a magnetic material. Magnetic nanostructured materials follow the Coulomb laws and can, therefore, be manipulated by an external magnetic field.[23]

The morphological analysis of Co-NPs by Transmission Electron Microscopy (TEM) showed that the nanoparticles have a spherical

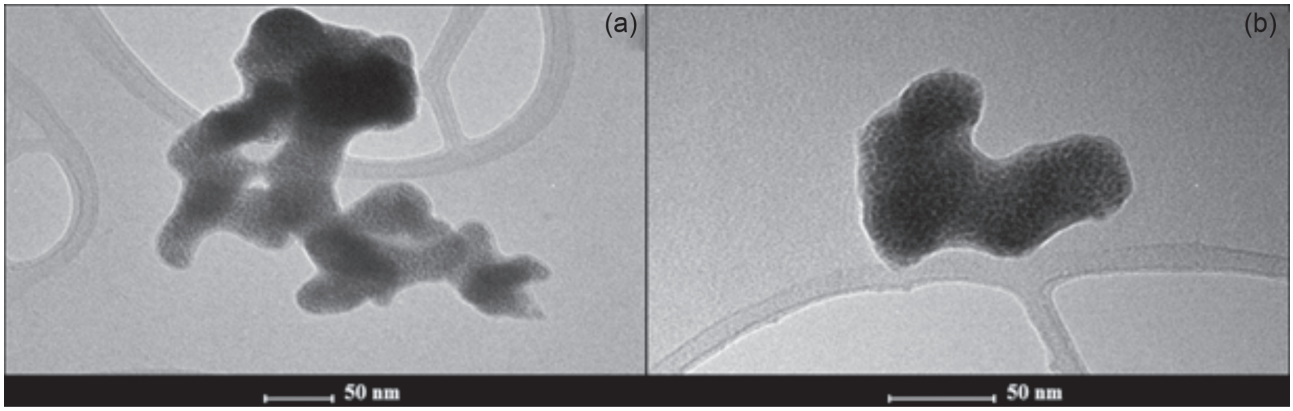

Figure 1. *Transmission Electron Microscopy of NPs-Co*

shape with a size of less than 50 nm (Figure 1). Since this material has high magnetic susceptibility,[23] the formation of agglomerates occurs.

Similar results are reported by Arshadi[24] which synthesized cobalt nanoparticles with spherical structures of 5-25 nm and Liang and Zhao[8] which synthesized NPs-Co with regular sizes around 10-20 nm.

The X-ray diffractogram of Co-NPs is shown in Figure 2. The diffraction peaks at 47.87° and 75.84° correspond to the metallic cobalt phase (JCPDS 5-727). The diffraction peaks at 34.7°, 39.55°, 57.2° and 68.6° correspond to cobalt oxide II (CoO) (JCPDS 42-1300). The peaks related to metallic cobalt were shown to be of low intensity, in relation to the reflections related to the CoO phase. This low intensity can be caused by the rapid oxidation of metallic cobalt under environmental conditions, which is due to its high magnetic susceptibility.[23]

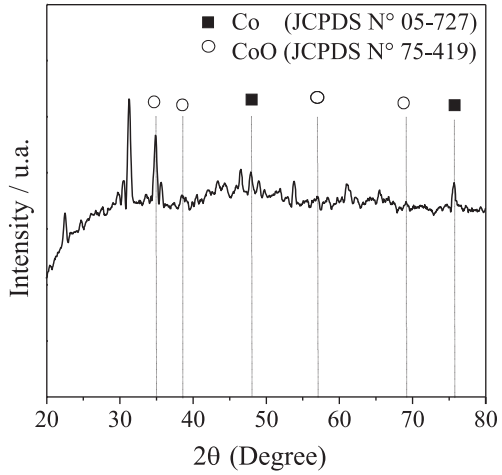

Figure 2. *X-ray diffractogram of NPs-Co*

Wang *et al.*,[2] used cobalt-coated bamboo charcoal. In their characterization by X-ray Diffraction, the authors obtained peaks at 44.22°, 51.54°, and 75.83° relative to metallic cobalt. The peak 75.83° is similar to that obtained in this work (75.84°). Matveev *et al.*,[25] used NPs-Co stabilized in polytetrafluoroethylene. In the analysis by X-ray Diffraction, peaks were obtained at 47.60° and 36.70° relative to cobalt metal and CoO, respectively. The peak 47.60° related to Co is similar to that obtained with the NPs-Co synthesized in this work (47.87°).

The The infrared analysis before and after the reaction can be observed in Figure 3.

The wide absorption bands in the region of 3500-3100 cm^{-1} can be attributed to the OH stretching vibration, and the band at 1636 cm^{-1} can be attributed to HOH binding vibration, indicating the presence

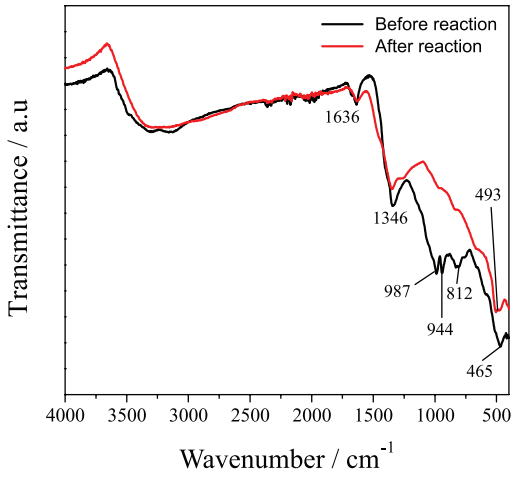

Figure 3. *Infrared spectrum: (–)NPs-Co before the reaction and (–)NPs-Co after the reaction.*

of hydroxyl groups and water molecules in the NPS-Co.[26] According to Liang and Zhao, [8] cobalt magnetic particles exhibit weak bonds between 525 and 831 cm^{-1}, which may be associated with Co^{2+}–O^{2-} stretching vibrations. These same bands were observed in this work. After the reaction it was observed that many peaks disappear and that some have moved and changes in intensity. This fact may be due to the chromium adsorption on the surface of the NPs-Co. Liu *et al.*,[27] in their work observed that after the adsorption of chromium there was displacement of some clusters.

The pH of the PZC was obtained from the arithmetic mean of the final pH values that showed a buffer effect (Figure 2S in Supplementary Material). The pH of the obtained PZC was 9.08. Thus at pH values below 9.08, the nanoparticles are positively charged and at pH above 9.08, the nanoparticles are negatively charged.

Influence of different parameters on Cr(VI) removal by Co-NPs

In order to verify the feasibility of the UV/Vis spectrophotometric method in the determination of Cr(VI) and Cr(III), some analytical parameters were analyzed as linear working range (LWR), limit of detection (LD), and limit of quantification (LQ) as can be seen in Table 1.

The first parameter to be evaluated in the Cr(VI) removal was the equilibrium time. From the Figure 4 it can be observed that there is a rapid removal of Cr(VI) in the first hours of reaction, increasing until approximately 8 hours, where the equilibrium is reached, removing about 90% of Cr(VI). However, the time of 10 hours was fixed for

Table 1. Analytical parameters of the Cr(VI) and Cr(III) determination method by UV/Vis Molecular Absorption Spectrophotometry

	LWR (mg L^{-1})	LD (mg L^{-1})	LQ (mg L^{-1})
Cr(VI)	0.500 to 40.0	0.284	0.946
Cr(III)	5.00 to 40.0	2.77	5.0

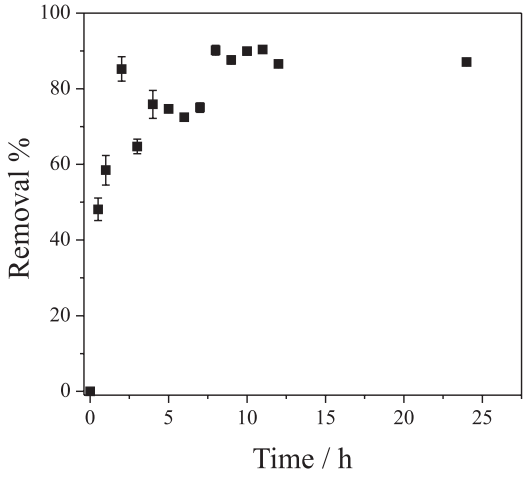

Figure 4. *Reactional equilibrium time between NPs-Co and Cr(VI). Experimental conditions: $C_{Cr(VI)}$ = 40.0 mg L^{-1}; volume of solution = 20.0 mL; system temperature = 25 ºC; dose of NPs-Co = 1.0 g L^{-1}; without pH adjustment (8.5); reaction time = 24 hours*

aliquot withdrawal in the subsequent experiments to ensure greater reliability that the equilibrium was achieved.

Once the equilibrium time was determined, the initial pH effect of the system on the Cr(VI) removal capacity was evaluated. It can be seen in the Figure 5A that the removal is favored at lower pH values. The removal percentage is about 100% at pH 2.0, whereas, at pH 12.00, the removal percentage is approximately 70%.

Initially, the adsorption process occurs due to electrostatic interactions between the anion chromate (CrO_4^{-2}) and the NPs-Co. Since at pH values below 9.08 the Co-NPs are positively charged, as determined by PZC, which will favor the Cr(VI) adsorption in the form of the chromate anion. With the increase of pH to values above PZC, the surface of the NPs will acquire a negative surface charge, reducing the adsorption of the chromate anion.

According to Figure 5B, it can be seen that there is an increase of the final pH independent of the initial pH of the system. In addition, a buffering of the system occurs at pH 9.0. This increase in pH is due to the release of OH^- ions into the reaction system due to the redox reactions occurring in aqueous solution (equations 4 and 5).

$$O_{2(g)} + 2H_2O_{(l)} + 4e^- \leftrightharpoons 4OH^-_{(aq)} \quad E°(V) = +0.40V \quad (4)$$

$$Co^{2+}_{(aq)} + 2e^- \leftrightharpoons Co_{(s)} \quad E°(V) = -0.280 \quad (5)$$

In addition to electrostatic interaction, oxidation reactions between Co-NPs and Cr(VI) species may also occur, since this process is thermodynamically favorable, as can be observed by the reduction potentials of equations 6 and 7.

$$CrO^{2-}_{4(aq)} + 8H^+_{(aq)} + 3e^- \leftrightharpoons Cr^{3+}_{(aq)} + 4H_2O_{(l)} \quad E°(V) = 1.33 \quad (6)$$

$$Co^{2+}_{(aq)} + 2e^- \leftrightharpoons Co_{(s)} \quad E°(V) = -0.280 \quad (7)$$

In order to verify if Cr(VI) reduces to Cr(III) during the removal process, the method of determining Cr(III) with EDTA was carried out. The Cr(III) was detected and quantified, and the Cr(III) concentration recovery was 110 ± 13%. It can be concluded, therefore, that all Cr(VI) was reduced to Cr(III).

Once Cr(VI) was found to be reduced in Cr(III), a species distribution graph was plotted as a function of pH (Figure 6) to verify which species predominated in solution. According to the species distribution graph, at pH 9.0, the $Cr(OH)_3$ fraction is approximately 0.9775. This indicates that Cr(III) is co-precipitated as $Cr(OH)_3$ in NPs-Co.

The influence of the initial concentration of Cr(VI) in the removal process by Co-NPs was investigated. As observed in Figure 7A, when the Cr(VI) concentration increases, a significant reduction in the removal rate occurs, which decreases from 80 to 15% when the concentration increases from 40.0 to 300.0 mg L^{-1}. This fact can be justified by the saturation of the active sites present in the NPs-Co at higher concentrations.

As noted in Figure 7B, the equilibrium removal ability increases with increasing Cr(VI) concentration, reaching approximately 50 mg g^{-1}. This phenomenon can be justified because of a greater interaction between the adsorbate and the nanoparticles. This would facilitate the transfer of Cr(VI) molecules in solution to the active sites of the nanoparticles, due to the increase in the motive force of the reaction medium and, consequently, resulting in an increase of the removal capacity.[28,29]

The dose effect of NPs-Co on the removal of Cr(VI) was also evaluated. As can be seen in Figure 8, with the increasing of the NPs-Co dose to 1.0 g L^{-1}, the Cr(VI) removal percentage is increased proportionally, reaching about 90% removal. From the 1.0 g L^{-1} dose, the system tends to equilibrate, reaching about 100% removal with

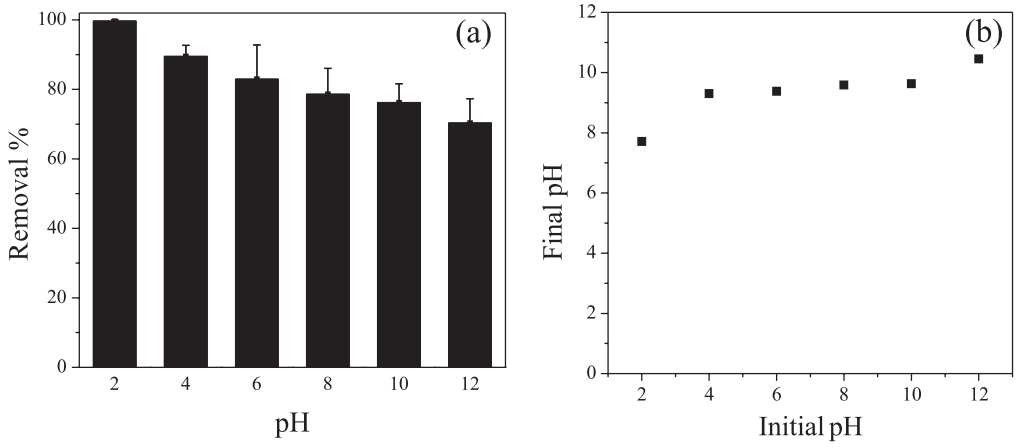

Figure 5. *(A) Removal of Cr(VI) at different pH values; (B) Relationship between initial pH × final pH. Experimental conditions: pH range 2.0 – 12.0; $C_{Cr(VI)}$ = 40.0 mg L^{-1}; volume of solution = 20.0 mL; system temperature = 25 ºC; dose of NPs-Co = 1.0 g L^{-1}; without pH adjustment; reaction time = 10 hours*

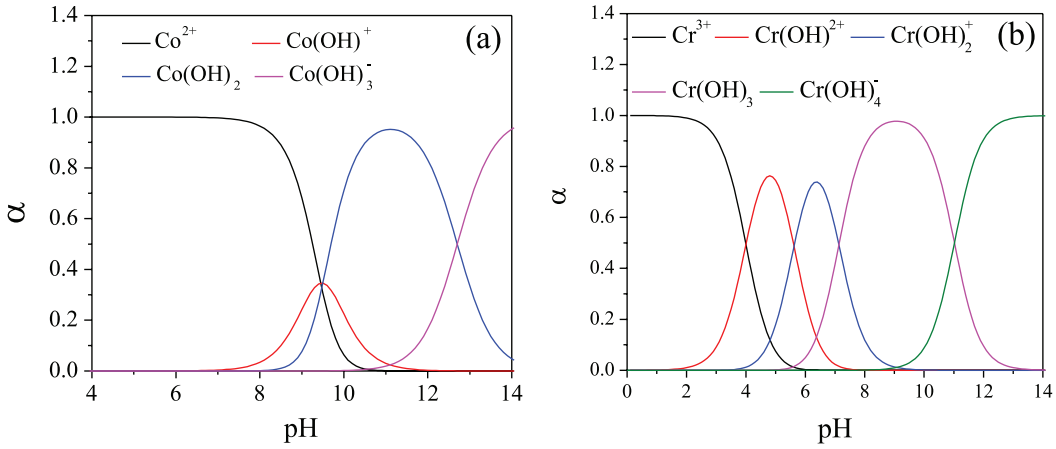

Figure 6. *System distribution pattern (a) cobalt (b) chromium. Graph generated with the spreadsheet TitGer*

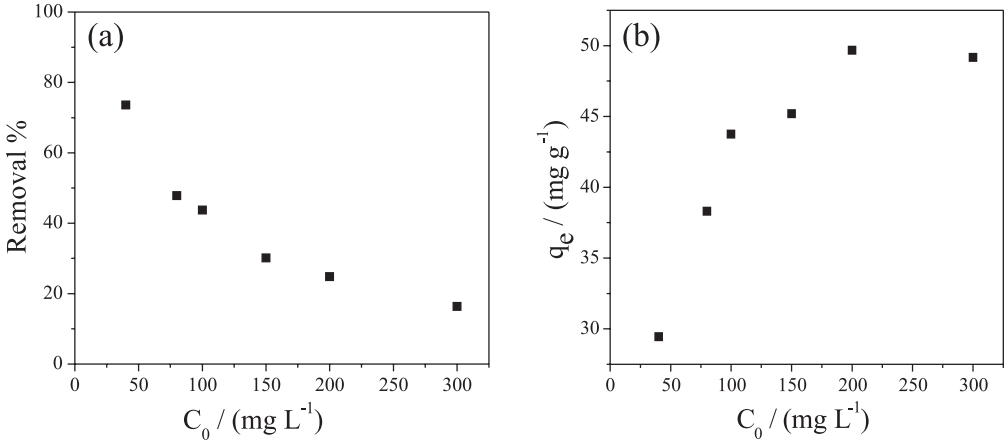

Figure 7. *(A) Effect of the initial concentration Cr(VI) on the removal process; (B) Effect of the initial concentration Cr(VI) on the removal capacity. Experimental conditions: $C_{Cr(VI)}$ = 40.0, 80.0, 100.0, 150.0, 200.0 and 300.0 mg L^{-1}; volume of solution = 20.0 mL; system temperature = 25 ºC; dose of NPs-Co = 1.0 g L^{-1}; without pH adjustment (8.5); reaction time = 10 hours*

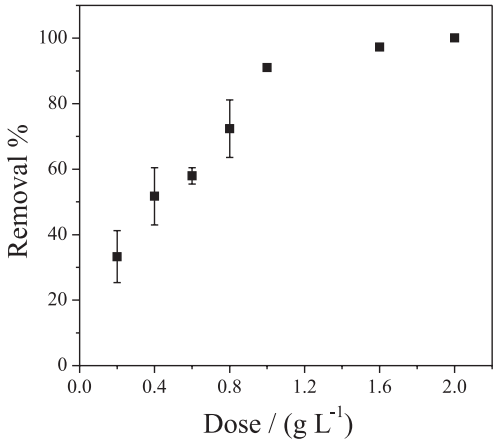

Figure 8. *Effect of the dose of NPs-Co on the removal of Cr(VI). Experimental conditions: $C_{Cr(VI)}$ = 40.0 mg L^{-1}; volume of solution = 20.0 mL; system temperature = 25 ºC; without pH adjustment (8.5); dose of NPs-Co = 1.0 g L^{-1}; reaction time = 10 hours*

the 2.0 g L^{-1} dose. The increase in Cr(VI) removal with increasing dose of Co-NPs may be due to the increase in total surface area and the availability of more adsorption sites.[30]

Kinetic studies of Cr(VI) removal by Co-NPs

The kinetics study of removal is very important as it provides important information about the pathways and mechanism of reactions.[31] The data were analyzed according to the equations of pseudo-first order (Equation 8) and pseudo-second order (Equation 9).

$$\log(q_e - q_t) = \log q_e - \left(\frac{k_1}{2.303}\right)t \quad (8)$$

$$\frac{t}{q_t} = \frac{1}{k_2 q_e^2} + \frac{t}{q_e} \quad (9)$$

wherein q_e (mg g^{-1}) and q_t (mg g^{-1}) are adsorption capacities of Cr(VI) at equilibrium time and at time t (hours), respectively; k_1 (g mg^{-1} min^{-1}) and k_2 (g mg^{-1} min^{-1}) are the pseudo-first order and pseudo-second order velocity constants, respectively.

The kinetic parameters of Cr(VI) removal by Co-NPs can be seen in Table 2. The kinetic model of pseudo-second order was better fitted to the experimental data as can be observed by the coefficient of determination (Figure 3S in Supplementary Material). In addition, the value of the maximum adsorption capacity obtained experimentally was 36.1 mg g^{-1}, a value very close to that found by the pseudo-second model that was equal to 36.90 mg g^{-1} displayed an error of 2.2%. This fact confirms the best fit of the pseudo-second model to the system studied.

Wang *et al.*,[2] promoted the removal of Cr(VI) in aqueous solution using cobalt-coated bamboo charcoal, and the best fit kinetic model was also the pseudo-second order, whose maximum adsorption capacity was 18.52 mg g^{-1}, about half that was obtained by the NPs-Co

Table 2. Kinetic parameters of Cr(VI) adsorption in magnetic NPs-Co

Pseudo-first order			Pseudo-second order		
K_1	q_e (mg g^{-1})	R^2	K_2	q_e (mg g^{-1})	R^2
0.4626	31.86	0.624	0.049	36.90	0.992

used in this work, which was 36.1 mg g^{-1}, demonstrating the efficiency of this nanoparticle in Cr(VI) removal.

Adsorption isotherms

The adsorption isotherms are used to propose a relationship between the adsorbed amount and the equilibrium solution at a fixed temperature.[31,32] The experimental data were adjusted to the Langmuir and Freundlich isotherm models, equations 10 and 11, respectively.

$$\frac{C_e}{q_e} = \frac{1}{q_{max}} C_e + \frac{1}{K_L q_{max}} \quad (10)$$

$$\log q_e = \log K_F + \frac{1}{n} \log C_e \quad (11)$$

wherein k_L is the equilibrium constant of the Langmuir model (L mg^{-1}), q_{max} (mg g^{-1}) is the maximum adsorption capacity, K_F is the isothermal constant of Freundlich (L g^{-1}) which is an approximation indicator of the adsorption capacity and n_F is the adsorption intensity that measures the deviation of the adsorption linearity.

The graphs of the experimental adjustments to the isotherms can be seen in the Figure 4S (in supplementary material), and the values of the parameters obtained by the Langmuir and Freundlich equations are shown in Table 3.

Table 3. Langmuir and Freundlich parameters for the process of Cr(VI) removal by NPs-Co

Langmuir			Freundlich		
K_L (L mg^{-1})	q_{max} (mg g^{-1})	R^2	K_F (L g^{-1})	$1/n_F$	R^2
0.0601	66.67	0.980	15.035	3.50	0.933

According to the data in Table 3, it is possible to observe that the Langmuir model was better fitted to the experimental data, whose coefficient of determination was 0.980, higher than that of Freundlich (0.950). The Langmuir adsorption model assumes that the adsorbate (Cr(VI)) distribution occurs in a monolayer on a surface, with a finite number of identical sites that are distributed homogeneously on the adsorbent surface.[30] In this case, adsorption is limited to one layer only, where all active sites are equal, i.e. the capacity of a molecule to occupy a given site is independent of the occupation of a neighboring site.[33]

The Langmuir parameters can be used to predict the affinity between adsorbent and adsorbent using the dimensionless separation factor (K_L). For values $0<K_L<1$ the adsorption is favorable.[34] According to the results obtained, the adsorption of Cr(VI) by Co-NPs is a favorable process, since the Langmuir constant obtained was 0.0601.

Adsorption studies of Cr(VI) by different adsorbents are shown in Table 4. It is possible to verify that the maximum adsorption capacity of Cr(VI) by the NPs-Co obtained in this work (66.67 mg g^{-1}) was superior to most of the adsorbents mentioned below.

Thermodynamic parameters

In order to evaluate the effect of temperature on Cr(VI) adsorption by Co-NPs, the thermodynamic parameters were determined by the Langmuir adsorption isotherm. The thermodynamic parameters, such as the change in Gibbs free energy (ΔG°, kJ mol^{-1}), enthalpy (ΔH°, kJ mol^{-1}), and entropy (ΔS°, J mol^{-1} K^{-1}) were determined.

From the calculated value of K_L at different temperatures (15, 25, 35, 45 and 55 °C) and by means of the Van't Hoff equation 12, it was possible to plot a graphic InK_L versus T^{-1}. The linear behavior allows the direct estimation of the thermodynamic parameters ΔS_{ads} and ΔH_{ads}, from the respective linear and angular coefficients. The achievement of ΔG_{ads} can be calculated from equation 13.

$$\ln K_L = \frac{\Delta S°}{R} - \frac{\Delta H}{RT} \quad (12)$$

$$\Delta G° = \Delta H° - T\Delta S° \quad (13)$$

wherein R (8.314 J mol^{-1} K^{-1}) is the ideal gas constant, T (K) is the temperature in Kelvin, and K_L (L mg^{-1}) is Langmuir constant. The thermodynamic parameters obtained for Cr(VI) removal by Co-NPs are shown in Table 5.

The negative values of ΔG ° presented in Table 5 confirm the viability of the adsorption process and its spontaneous nature, which potentiates the use of the adsorbent in conventional processes of decontamination of Cr(VI) containing waters or effluents.[41] In addition, a reduction of this parameter occurs as the temperature increases, that is, it is confirmed that the adsorption is favored by

Table 4. Comparison of adsorption capacities of Cr(VI) by different adsorbents

Adsorbents	q_e (mg g^{-1})	Isotherm	Reference
NPs-Co	66.6	Langmuir	Actual
Cobalt-coated bamboo charcoal	38.46	Langmuir	2
Gross dolomite	10.01	Freundlich	35
Coconut shell fibers	29.0	Langmuir	36
Maghemite (γ-Fe_2O_3)	19.2	Freundlich	37
Activated charcoal	3.46	Langmuir	38
Activated Carbon	28.02	Langmuir/Freundlich	39
Nanoscale Fe^0 on graphene nanosheet	21.72	Langmuir	3
Nanoscale Fe^0 assembled on magnetic Fe_3O_4/graphene	101.0	Langmuir	6
Activated carbon prepared from longan seed	169.49	Langmuir	40
Waste pomace of olive oil	18.69	Langmuir	34

Table 5. Thermodynamic parameters for the removal of Cr(VI) by NPs-Co

T (°C)	Thermodynamic parameters		
	ΔG° (kJ mol^{-1})	ΔH° (kJ mol^{-1})	ΔS° (J mol^{-1} K^{-1})
15 °C	- 18.4		
25 °C	- 19.3		
35 °C	- 20.6	4.88	81.0
45 °C	- 20.9		
55 °C	- 21.7		

the increase in temperature. Negative values for ΔG° accompanied by positive values for ΔS° indicate that the adsorption process is spontaneous and that the adsorbent has an affinity for the adsorbate.[42]

The positive value of ΔH° indicates that the adsorption process was of an endothermic nature, as previously reported, due to the increase in adsorption capacity with increasing temperature. The positive value of ΔS° suggests the likelihood of a favorable adsorption and an increase in the randomnes of the solid/solute interface where the adsorption occurred.[39,43]

Similar results were obtained in other works. Yang *et al*.,[40] promoted the adsorption process of Cr(VI) by activated carbon prepared from longan seed, in which the adsorption was more efficient at higher temperatures, i.e. endothermic process, with a value of ΔH° obtained was 2.73 kJ mol^{-1}, close to the value obtained in this work. Malkoc *et al*.,[34] used as adsorbent waste pomace of olive oil in adsorption of Cr(VI) and calculated the ΔH° and ΔS° as being equal to 11.84 kJ mol^{-1} and 34.80 J mol^{-1} K^{-1} respectively. The values of ΔG° obtained showed that an increase of the spontaneity occurs with the increase in temperature since ΔG° decreases with the increase of the temperature.

Desorption and reuse assays of NPs-Co

After reaction of Co-NPs with Cr(VI), the desorption of chromium was carried out. The quantification of desorbed total chromium was performed using Flame Atomic Absorption. The results indicated that only 10% of the total chromium removed was desorbed.

Wang *et al*.,[2] used cobalt-coated bamboo charcoal, the authors were able to desorb about 98% of the chromium adsorbed under alkaline conditions.

To evaluate the reuse of NPs-Co, three consecutive adsorption/desorption cycles were done. The results indicated that the first cycle showed a Cr(VI) removal of approximately 80%, which was reduced to 26% in the second cycle and 23% in the third cycle. This low percentage of removal in the reuse of Co-NPs may be associated with the low desorption index. According Wang *et al*., [2] the cobalt-coated bamboo charcoal can be used in five cycles.

Removal Mechanism of Cr(VI) by NPs-Co

The Cr(VI) removal process by Co-NPs occurs initially by the adsorption of the Cr(VI) species on the surface of NPs-Co, due to the electrostatic interactions between the positively charged adsorbent and the anion CrO_4^{2-}. In the sequence Cr(VI) is reduced to Cr(III). With an elevation of the pH of the system, $Cr(OH)_3$ formation occurs, whose species are co-precipitated under the surface of the NPs-Co.

CONCLUSION

The NPs-Co were synthesized by the chemical reduction method with sodium borohydride, in a simple and fast, presented magnetic properties and nanometric size, less than 50 nm. This material was used in the Cr(VI) removal process in aqueous solutions, proving highly efficient, reaching approximately 90% removal in 10 hours of reaction. The NPs-Co has the advantage of being magnetic and can be easily removed from the system by applying a magnetic field. The adsorption process was best described by the Langmuir model with maximum adsorption capacity of 66.6 mg g^{-1}. The kinetic model of pseudo-second order was better fitted to the experimental data than to pseudo-first order. The thermodynamic study showed that the adsorption was of an endothermic and spontaneous nature, thus being a viable method to be applied.

SUPPLEMENTARY MATERIAL

Supplementary data (Figure NPs-Co in the presence of an external magnetic field; Point zero charge of NPs-Co; Removal kinetics of the Cr(VI) adjusted to the pseudo-first order and pseudo-pseudo-second order; Langmuir and Freundlich isotherm).

ACKNOWLEDGMENT

The authors thank the financial support from Coordenação de Aperfeiçoamento de Pessoal de Nível Superior - Brasil (CAPES) - Finance Code 001, Conselho Nacional de Desenvolvimento Científico e Tecnológico (CNPq), Fundação de Amparo à Pesquisa do Estado de Minas Gerais (FAPEMIG), CNPq/FAPEMIG (agreement recorded in SICONV: 793988/2013). Also, thank the Microscopy Center at the Universidade Federal de Minas Gerais (http://www.microscopia.ufmg.br) for providing the equipment and technical support for the experiments involving electron microscopy.

REFERENCES

1. Rosenberg, E.; Johnson Matthey Tech **2015**, *59*, 293.
2. Wang, Y.; Wang, X. J.; Liu, M.; Wang, X.; Wu, Z.; Yang, L. Z.; Xia, S. Q.; Zhao, J. F.; *Ind Crops Prod.* **2012**, *39*, 81.
3. Li, X.; Ai, L.; Jiang, J.; *Chem. Eng. J.* **2016**, *288*, 789.
4. Jin, J.; Yang, Z.; Xiong, W.; Zhou, Y.; Xu, R.; Zhang, Y.; Cao, J.; Li, X.; Zhou, C.; *Sci. Total Environ.* **2019**, *650*, 408.
5. Geng, B.; Jin, Z.; Li, T.; Qi, X.; *Chemosphere* **2009**, *75*, 825.
6. Lv, X.; Xue, X.; Jiang, G.; Wu, D.; Sheng, T.; Zhou, H.; Xu, X.; *J. Colloid Interface Sci.* **2014**, *417*, 51.
7. Yi, Y.; Tu, G.; Eric Tsang, P.; Xiao, S.; Fang, Z.; *Mater. Lett.* **2019**, *234*, 388.
8. Liang, X.; Zhao, L.; *RSC Adv.* **2012**, *2*, 5485.
9. Naz, S.; Khaskheli, A. R.; Aljabour, A.; Kara, H.; Talpur, F. N.; Sherazi, S. T. H.; Khaskheli, A. A.; Jawaid, S.; *Adv. Chem.* **2014**, *ID 686925*.
10. Sha, Y.; Mathew, I.; Cui, Q.; Clay, M.; Gao, F.; Zhang, X. J.; Gu, Z.; *Chemosphere* **2016**, *144*, 1530.
11. Zola, A. S.; Ribeiro, R. U.; Bueno, J. M. C.; Zanchet, D.; Arroyo, P. A.; *J Exp Nanosci.* **2014**, *9*, 398.
12. Bibi, I.; Nazar, N.; Iqbal, M.; Kamal, S.; Nawaz, H.; Nouren, S.; Safa, Y.; Jilani, K.; Sultan, M.; Ata, S.; Rehman, F.; Abbas, M.; *Adv. Powder Technol.* **2017**, *28*, 2035.
13. Ravi Dhas, C.; Venkatesh, R.; Jothivenkatachalam, K.; Nithya, A.; Suji Benjamin, B.; Moses Ezhil Raj, A.; Jeyadheepan, K.; Sanjeeviraja, C.; *Ceram. Int.* **2015**, *41*, 9301.
14. Warang, T.; Patel, N.; Fernandes, R.; Bazzanella, N.; Miotello, A.; *Appl Catal B.* **2013**, *132-133*, 204.
15. Calvete, T.; Lima, E. C.; Cardoso, N. F.; Dias, S. L. P.; Pavan, F. A.; *Chem. Eng. J.* **2009**, *155*, 627.
16. Giacomni, F.; Menegazzo, M. A. B.; Silva, M. G. d.; Silva, A. B. d.; Barros, M. A. S. D.; *Revista Matéria* **2017**, *22*.

17. http://www.merckmillipore.com/INTERSHOP/web/WFS/Merck-JP-Site/ja_JP/-/JPY/ShowDocument-Pronet?id=201702.131, acessado em 29/04/2019
18. Lagergren, S.; *Handlingar* **1898**, *24*, 39.
19. Ho, Y. S.; McKay, G.; *Resour Conserv Recy* **1999**, *25*, 171.
20. Langmuir, I.; *J. Am. Chem. Soc.* **1918**, *40*, 1361.
21. Langmuir, I.; *J. Am. Chem. Soc.* **1916**, *36*, 1.
22. Freundlich, H. M. F.; *J Phys Chem* **1906**, 385.
23. Sargentelli, V.; Ferreira, A. P.; *Eclét. Quím.*, **2010**, *35*, 153.
24. Arshadi, M.; *J. Mol. Liq.* **2015**, *211*, 899.
25. Matveev, V. V.; Baranov, D. A.; Yurkov, G. Y.; Akatiev, N. G.; Dotsenko, I. P.; Gubin, S. P.; *Chem. Phys. Lett.* **2006**, *422*, 402.
26. Xiong, L.; Chen, C.; Chen, Q.; Ni, J.; *J Hazard. Mater* **2011**, *189*, 741.
27. Liu, W.; Chen, H.; Borthwick, A. G. L.; Han, Y.; Ni, J.; *Chem. Eng. J.* **2013**, *232*, 228.
28. Gautam, R. K.; Rawat, V.; Banerjee, S.; Sanroman, M. A.; Soni, S.; Singh, S. K.; Chattopadhyaya, M. C.; *J. Mol. Liq.* **2015**, *212*, 227.
29. Shu, J.; Wang, Z.; Huang, Y.; Huang, N.; Ren, C.; Zhang, W.; *J. Alloys Compd.* **2015**, *633*, 338.
30. Kataria, N.; Garg, V. K.; Jain, M.; Kadirvelu, K.; *Adv. Powder Technol.* **2016**, *27*, 1180.
31. Baniamerian, M. J.; Moradi, S. E.; Noori, A.; Salahi, H.; *Appl. Surf. Sci.* **2009**, *256*, 1347.
32. El-Bindary, A. A.; Diab, M. A.; Hussien, M. A.; El-Sonbati, A. Z.; Eessa, A. M.; *Spectrochim Acta A Mol Biomol Spectrosc.* **2014**, *124*, 70.
33. Febrianto, J.; Kosasih, A. N.; Sunarso, J.; Ju, Y.-H.; Indraswati, N.; Ismadji, S.; *J. Hazard. Mater* **2009**, *162*, 616.
34. Malkoc, E.; Nuhoglu, Y.; Dundar, M.; J. ;*Hazard. Mater* **2006**, *138*, 142.
35. Albadarin, A. B.; Mangwandi, C.; Al-Muhtaseb, A. a. H.; Walker, G. M.; Allen, S. J.; Ahmad, M. N. M.; *Chem. Eng. J.* **2012**, *179*, 193.
36. Demiral, H.; Demiral, İ.; Tümsek, F.; Karabacakoğlu, B.; *Chem. Eng. J.* **2008**, *144*, 188.
37. Hu, J.; Chen, G.; Lo, I. M. C.; *Water Res.* **2005**, *39*, 4528.
38. Selvi, K.; Pattabhi, S.; Kadirvelu, K.; *Bioresour. Technol.* **2001**, *80*, 87.
39. Acharya, J.; Sahu, J. N.; Sahoo, B. K.; Mohanty, C. R.; Meikap, B. C.; *Chem. Eng. J.* **2009**, *150*, 25.
40. Yang, J.; Yu, M.; Chen, W.; *J Ind Eng Chem.* **2015**, *21*, 414.
41. Hu, X.-j.; Wang, J.-s.; Liu, Y.-g.; Li, X.; Zeng, G.-m.; Bao, Z.-l.; Zeng, X.-x.; Chen, A.-w.; Long, F.; *J. Hazard. Mater* **2011**, *185*, 306.
42. Nascimento, R. F. d.; Lima, A. C. A. d.; Vidal, C. B.; Melo, D. d. Q.; Raulino, G. S. C.; Em *Adsorção: aspectos teóricos e aplicações ambientais,* ed. Imprensa Universitária. 2014.
43. Gupta, S.; Babu, B. V.; *Chem. Eng. J.* **2009**, *150*, 352.